Journal of Crystal Growth 312 (2010) 263–266

Contents lists available at ScienceDirect

Journal of Crystal Growth

journal homepage: www.elsevier.com/locate/jcrysgro

Metastable rocksalt ZnO interfacial layer and its influence on polarity selection of Zn-polar ZnO films

H.T. Yuan [a,*], Y.Z. Liu [a], Z.X. Mei [a], Z.Q. Zeng [a], Y. Guo [a], X.L. Du [a,*], J.F. Jia [b], Z. Zhang [c], Q.K. Xue [b]

[a] Beijing National Laboratory for Condensed Matter Physics, Institute of Physics, Chinese Academy of Sciences, Beijing 100190, China
[b] Department of Physics, Tsinghua University, Beijing 100084, China
[c] Beijing University of Technology, Beijing 100022, China

ARTICLE INFO

Article history:
Received 27 June 2009
Received in revised form
11 October 2009
Accepted 23 October 2009
Communicated by E. Calleja
Available online 31 October 2009

PACS:
61.14.Hg
68.37.Lp
68.35.Ct
68.35.Rh

Keywords:
A1. Interface
A1. Metastable structure
A1. Planar defects
A1. Phase equilibrium
A3. Molecular beam epitaxy

ABSTRACT

By a metastable rocksalt ZnO interfacial structure and a resulting rocksalt-to-wurtzite structure transition in ZnO buffer layer, polarity control of Zn-polar ZnO films was realized on rocksalt MgO (1 1 1) template by plasma-assisted molecular beam epitaxy. The metastable rocksalt ZnO and the phase transition from octahedrally bonded rocksalt to tetrahedrally bonded wurtzite structure during the growth of ZnO buffer layer were established by the combination of *in situ* reflection high-energy electron diffraction and *ex situ* high-resolution transmission electron microscopy. Such a metastable rocksalt ZnO has a lattice constant a=4.16 Å and a typical …*abcabc*… atom stacking along the growth direction. Polarity selection of Zn-polar ZnO films was found greatly depending on the bonding configuration of the epitaxial ZnO interfacial layer, and an atomic model of the structure transition was proposed to explain the mechanism of ZnO polarity selection.

1. Introduction

As a wide band-gap semiconductor with a large exciton binding energy of 60 meV, the hetero-epitaxial growth of ZnO films has attracted extensive attention due to the potential applications for short-wavelength optoelectronic devices [1,2]. In thermodynamically stable wurtzite ZnO structure, the lack of an inversion symmetry center along the *c*-axis results in the formation of two polar surfaces: O-polar and Zn-polar. Two polar surfaces are known to be structurally and chemically different, which leads to many variations in their properties such as photoluminescence [3], impurity incorporation [4], as well as spontaneous polarization [5] and surface morphology [6]. More importantly, the unipolar ZnO films make the design and fabrication of some special ZnO devices and nanostructures available. For example, high-mobility two-dimensional electron gas (2DEG) induced by the spontaneous polarization of wurtzite ZnO was achieved in O-polar ZnO/ZnMgO heterostructure, where quantum Hall effect could be clearly observed in the heterojunction at low temperature [7]. Therefore, from the point view of both technological applications and fundamental researches, polarity-controlled epitaxy of unipolar ZnO films is of practical interest.

Recently, the controlled growth of unipolar ZnO films has been realized by interface engineering using MgO buffer layer on α-Al_2O_3 (0 0 0 1) and $MgAl_2O_4$ (1 1 1) substrates [6,8–11]. Phase structures of the MgO buffer layers have been found to have an immediate effect on the polarity control of ZnO films. On α-Al_2O_3 (0 0 0 1) surface, an ultrathin MgO buffer layer with wurtzite structure resulted in O-polar ZnO films, while, the rocksalt MgO buffer layer was supposed to lead to Zn-polar ZnO films [6,8–10]. Nevertheless, as a matter of fact, before the final establishment of the polarity of ZnO films, an additional ZnO buffer layer is always used just following the growth of MgO buffer layer to further decrease the interface strain from lattice mismatch. Normally, this ZnO buffer layer shows a typical tetrahedral wurtzite structure. Whereas, sometimes, under the influence of the lattice-mismatch

* Corresponding authors: Tel.: +86 10 82649035; fax: +86 10 82649228.
E-mail addresses: h.t.yuan.hongtao@gmail.com (H.T. Yuan).
xldu@aphy.iphy.ac.cn (X.L. Du).

0022-0248/$ - see front matter © 2009 Elsevier B.V. All rights reserved.
doi:10.1016/j.jcrysgro.2009.10.054

strain from underlied rocksalt MgO template, ZnO buffer layer also can adopt an octahedral rocksalt structure. Theoretically, the possibility of ZnO structure transition from wurtzite (WZ) to rocksalt (RS), especially under high pressure conditions, has been reported in the literatures [12–15]. However, experimentally, very little is known so far about the ZnO phase structures at strain-accumulated interfaces, and their influence on polarity control of the unipolar epitaxial ZnO films.

In this study, a metastable rocksalt ZnO structure in strained interface and a structure transition from rocksalt-to-wurtzite ZnO were observed during the epitaxial growth of ZnO buffer layers on rocksalt MgO (1 1 1) template. The well-defined polarity of unipolar ZnO film was determined using convergent beam electron diffraction (CBED) technique. It was found that ZnO structure transition from the octahedral rocksalt to the tetrahedral wurtzite played a vital role on the polarity selection of Zn-polar ZnO films grown on octahedrally bonded MgO templates. Combined with *in situ* reflection high-energy electron diffraction (RHEED) and cross-sectional high-resolution transmission electron microscopy (HRTEM), the interfacial microstructures of ZnO buffer layers were investigated. An atomistic model is proposed to understand the ZnO structure transition and the influence of metastable rocksalt ZnO on the achievement of Zn-polar ZnO films.

2. Experimental details

Using rocksalt MgO buffer layers on α-Al_2O_3 (0 0 0 1) and $MgAl_2O_4$ (1 1 1) substrates, as well as directly on MgO (1 1 1) surfaces, unipolar ZnO films were prepared by the interfacial engineering using plasma-assisted molecular beam epitaxy. Element zinc (7N grade), magnesium (5N grade) and oxygen plasma (radio frequency, O_2 gas over 5N grade) were used as beam sources. The substrates were degreased, acid-etched and then thermally cleaned at 800 °C in UHV for 30 min. Prior to growth, the substrate was exposed to the oxygen plasma with a radio frequency power of 400 W and a gas flux of 2.0 ccm for 30 min to obtain smooth O-terminated surfaces. Then, whichever substrate is used, the rocksalt MgO buffer layer was grown along the [1 1 1] direction with a rate of 1.0 nm/min under an O-rich situation, in which, the defect-free and stoichiometric MgO could be obtained as the reproducible template for ZnO epitaxy. After 2.5 min growth of MgO, an annealing process was followed to improve its surface smoothness. Afterward, on this annealed rocksalt MgO template, low-temperature ZnO buffer layer was grown at 380 °C with a slow rate of 0.8 nm/min for 10 min, during which, firstly the metastable rocksalt ZnO and then the structure transition from rocksalt-to-wurtzite phase were clearly observed by *in situ* RHEED observations. After an annealing process at 750 °C for 3 min, the epitaxial growth of unipolar ZnO film started at 650 °C. It is addressed that all our RHEED observations are performed in the *in situ* and real-time mode without changing any observation parameter.

3. Results and discussion

Fig. 1 shows the evolution of RHEED patterns during the epitaxial growth of ZnO buffer layer on MgO (1 1 1) template, with incidence electron beam along MgO$\langle 1\bar{1}0\rangle$ azimuth. A clear RHEED pattern of single-domain rocksalt MgO without any twinning crystal, obtained on $MgAl_2O_4$ (1 1 1) surface, is shown in Fig. 1(a). From the geometry of the diffraction spots, no *m* symmetry but only a simple two-fold symmetry can be observed, which strongly suggests the single-domain rocksalt MgO

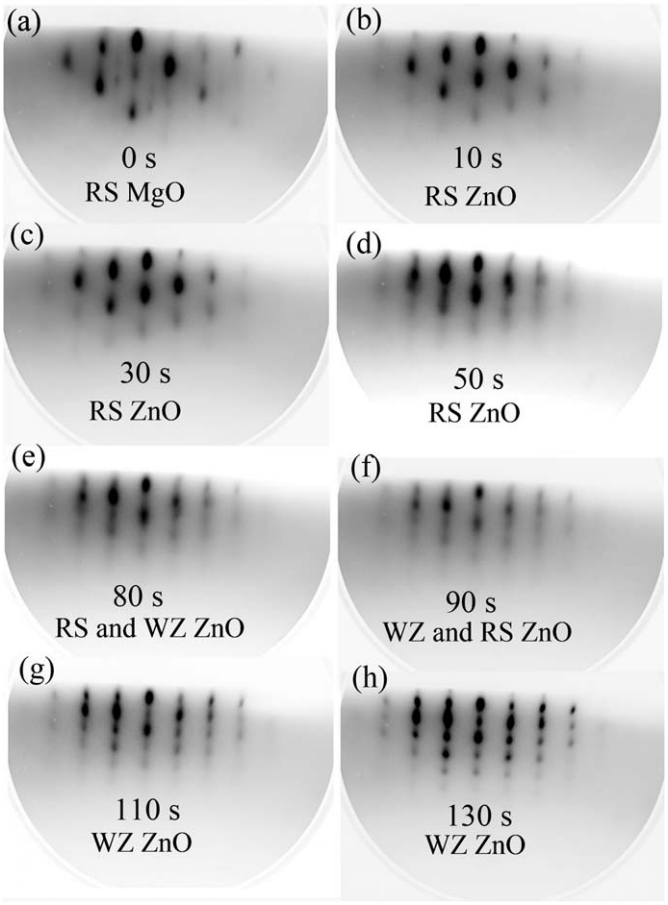

Fig. 1. RHEED pattern evolution during the growth of ZnO buffer layer, with incidence electron beam along MgO$\langle 1\bar{1}0\rangle$ azimuth. (a) Rocksalt MgO (1 1 1), (b) rocksalt ZnO (1 1 1) at 10 s, (c) 30 s, (d) 50 s, (e) mixed pattern of RS-ZnO (1 1 1) and WZ-ZnO (0 0 0 1) at 80 s, (f) mixed pattern of RS-ZnO (1 1 1) and WZ-ZnO (0001) at 90 s, (g) WZ-ZnO (0 0 0 1) at 110 s and (h) WZ-ZnO (0 0 0 1) at 130 s.

structure without twinning [16]. The good crystallization without twinning domain boundary makes this MgO buffer layer a good template to study the structure transformation of the following ZnO buffer layers. When the growth of ZnO buffer layer begins, changes happen in the relative intensity of the diffraction spots. As presented in Fig. 1(b), some spots are found obviously brighter than before. Whereas, compared to the geometry of rocksalt MgO patterns, no position change in ZnO pattern can be observed, which indicates that the as-grown ZnO overlayer still kept the rocksalt structure. The spotty patterns of ZnO suggest that the epitaxial growth of rocksalt ZnO buffer layer is in a typical three-dimensional island mode. In the following 40 s, these spotty patterns keep the uniform intensity and do not change too much, as displayed in Fig. 1(c) and (d). Note that, at the very beginning stage of the growth of ZnO buffer layer, where the coverage of ZnO on MgO is less than 1 (coverage $\theta < 1$), the observed RHEED pattern is a typical superposed pattern composed of the signals from both MgO surface and ZnO buffer. The origin of RHEED pattern partially comes from MgO template surface and strongly depends on the ZnO coverage before the MgO surface is fully covered. However, from the pattern between Fig. 1(a) (only MgO surface) and Fig. 1(b) (MgO surface partially covered by ZnO island), a clearly contrasting character can be observed: the related intensity between reflection spots is changing. Without any doubt, this changing comes from the newly grown ZnO islands. The changing in relative intensity of diffraction spots shown in Figs. 1(a)–(c) demonstrate the

phenomenon: when we grow ZnO slowly on MgO surface, the grown ZnO keeps the MgO structure at the first stage, by showing a RHEED pattern with relative changing in spot intensity and without changing the symmetry of diffraction spots.

After 50 s growth from the very beginning, one can see that the diffraction spots in Fig. 1(d) become a little blurred and elongated. At the 80th second, a new set of broad-and-blurred streaky pattern forms and imposes onto the original spotty one, as shown in Fig. 1(e). It can be found that the rod spacing of the new pattern is about 3.5% smaller than that of the above-mentioned metastable rocksalt ZnO structure. At the same time, the *m* symmetry can be deduced from the new ZnO pattern. In Fig. 1(f), the new streaky pattern is greatly reinforced and can be determined as a set of wurtzite ZnO pattern. From the RHEED observations, we could learn that the structure transition of ZnO from rocksalt to wurtzite began at the 80th second, and finished within the following 20 s. Most importantly, as shown in Figs. 1(b)–(d), the pattern corresponding to the rocksalt ZnO growth can be kept as long as about 80 s during the slow growth of ZnO buffer layer, indicating that the metastable rocksalt ZnO can be grown for about 80 s before the onset of the transition from rocksalt ZnO to wurtzite ZnO growth. With the known growth time and growth rate, we can figure out the thickness of this rocksalt ZnO buffer layer—around 1 nm (3–5 Zn–O bilayers along rocksalt ZnO [1 1 1] direction, consistent with the HRTEM results discussed later). The broad streaky pattern of wurtzite ZnO at the 110th second, as presented in Fig. 1(g), indicates that the growth of ZnO buffer layer gradually transfers from the three-dimensional mode to the quasi layer-by-layer mode after the structure transformation. The pattern in Fig. 1(h) reveals a typical wurtzite ZnO phase after the growth of 130 s.

In order to figure out the well-defined polarities of the as-grown ZnO films, HRTEM studies were carried out. In comparison with the dark field images of $g = \pm(0\,0\,0\,2)$ and the primary beam parallel to $[1\,1\,\bar{2}\,0]_{ZnO}$ zone axis, shown in Figs. 2(a) and (b), one can see that there is no inversion domain in the obtained ZnO film. The polarity of this unipolar ZnO film can be determined by comparing the experimental CBED pattern of 160-nm-thick ZnO sample with a series of simulated patterns of ZnO with different thicknesses. The experimental patterns are taken along the $[1\,0\,\bar{1}\,0]$ zone axis, and the calculated ones are simulated in the same direction. Since the CBED patterns of the as-grown ZnO sample (Fig. 2(c)) agree well with the simulated pattern of Zn-polar ZnO film with the same thickness of 160 nm (Fig. 2(d)), we can judge from the simulated pattern that the polarity of the wurtzite ZnO (WZ-ZnO) film grown on RS-ZnO/RS-MgO/substrate template is Zn-polar with the orientation along [0 0 0 1] direction, in accordance with the CBED studies in Refs. [6,9].

Microscopic interfacial structure of ZnO on RS-MgO (1 1 1)/$MgAl_2O_4$ (1 1 1) was investigated by high-resolution transmission electron microscopy. HRTEM image near the interface along $MgAl_2O_4[1\,0\,\bar{1}]$ zone axis is shown in Fig. 3. Fast Fourier transform image of the selected area in this interface between the $MgAl_2O_4$ spinel substrate and the wurtzite ZnO film, indicated by white arrows, clearly displays a parallelogram primitive unit cell in reciprocal lattice and a typical two-fold symmetry in diffraction geometry, which suggests that this layer has a rocksalt structure. In fact, inside this rocksalt structure, we still can find another sharp interface which obviously departs the rocksalt layer into two parts. By the growth rate and corresponding growing time of MgO and ZnO buffers, the interface can be determined as the boundary between the rocksalt MgO and the rocksalt ZnO. The thickness of the rocksalt MgO (RS-MgO) layer is about 2.5 nm and that of the rocksalt ZnO (RS-ZnO) is a little more than 1 nm. Stacking sequence in rocksalt ZnO along [1 1 1] direction is a typical …*abcabc*… order and the measured stacking period is 7.2 Å, from which we can deduce the basic lattice parameter *a* of the strained cubic ZnO as 4.16 Å. The formation of this metastable RS-ZnO is directly influenced by the RS-MgO template since the rocksalt ZnO almost completely succeeds the lattice parameters of the rocksalt MgO. Furthermore, due to the great strain caused by the two interfaces of WZ-ZnO/RS-ZnO and RS-ZnO/RS-MgO, some

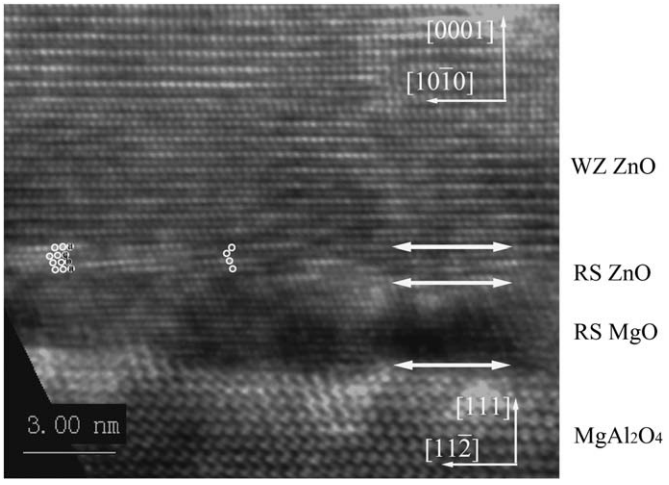

Fig. 3. HRTEM image near the interface along $MgAl_2O_4[1\,0\,\bar{1}]$ zone axis. Inside the rocksalt layer, both RS-MgO and metastable RS-ZnO have the similar crystal parameter d_{111} of 7.21 Å. The interfacial strain caused by lattice mismatch is released in rocksalt ZnO layer by the formation of the regular stacking faults. There is almost no stress in stable wurtzite ZnO epilayer.

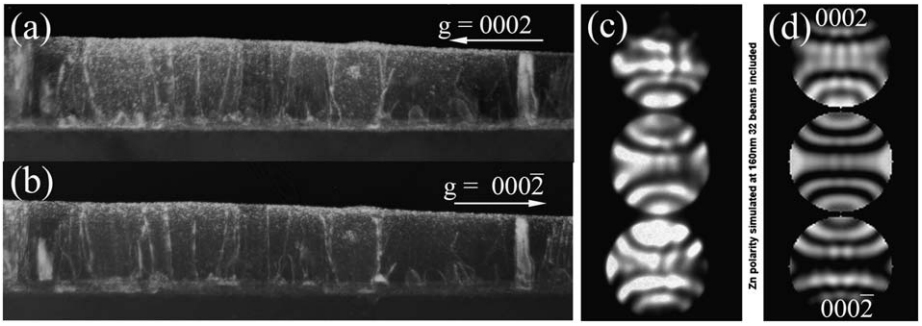

Fig. 2. Polarity measurement of the obtained wurtzite ZnO films on WZ-ZnO/RS-ZnO/RS-MgO template: (a) and (b) the dark filed images of $g = \pm(0\,0\,0\,2)$ with the primary beam parallel to $[1\,1\,\bar{2}\,0]_{ZnO}$ zone axis, (c) the experimental CBED pattern of 160-nm-thick ZnO sample and (d) the simulated CBED pattern of ZnO film with the same thickness as that of (c).

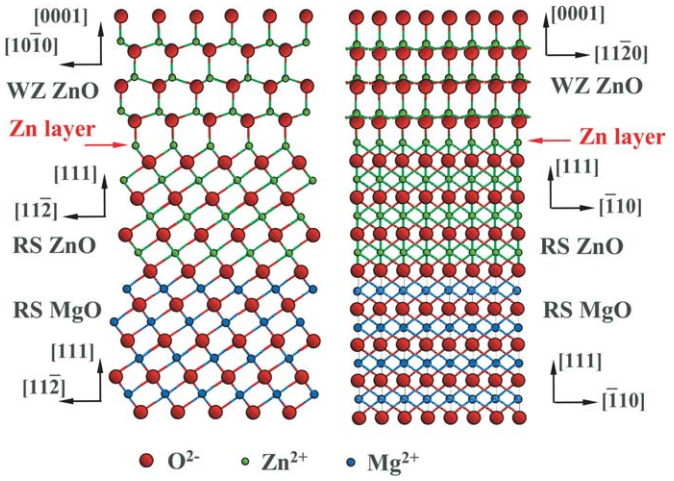

Fig. 4. A schematic diagram of the polarity selection of ZnO on rocksalt MgO template. The Zn–O bonding of Zn layer in RS-ZnO firstly erects upright to form the wurtzite ZnO structure with Zn-polar.

stacking faults regularly appear in rocksalt ZnO layer. These regular stacking faults released most of the interfacial strain and resultantly, the wurtzite ZnO above the RS-ZnO is found relaxed into the unstrained wurtzite ZnO structure.

It has been revealed that polarity selection of ZnO film strongly depends on phase structures of MgO buffer layers [6]. Since the wurtzite MgO structure has a polarity itself, ZnO films grown on such an MgO template with the O-polar wurtzite structure, will finally continue the polarity of wurtzite MgO [6]. However, polarity selection of the ZnO films grown on rocksalt MgO template is quite different because there is the structure transition in the inserted ZnO buffer layer before the polarity of stable wurtzite ZnO film is established. In our experiments, the rocksalt MgO layer was more important to serve as a growth template than play a role in polarity control. More importantly, the polarity selection of ZnO films on RS-MgO template is proposed to occur in ZnO buffer rather than in MgO buffer layer. As shown in Fig. 4, in the growth direction of the octahedrally bonded rocksalt ZnO, there are three bonds up and three bonds down for both Zn and O atoms. In order to transfer to a tetrahedrally bonded wurtzite structure, three tilted-up-bonds on the growing surface of RS-ZnO have to relax into one upright bond, which will lead to the symmetry breakage along the growth direction. Remarkably, the layer (Zn-layer or O-layer) whose bonding firstly erects upright will directly decide the polarity of the resulting wurtzite ZnO structure. If it happens in Zn layer, the wurtzite ZnO will be Zn-polar, while, if it happens in O layer, then O-polar. It can be speculated that it is at the Zn layer of rocksalt ZnO that the three tilted-up-bonds changes to one upright bond which results in the tetrahedrally bonded wurtzite structure. Our further theoretical investigations are in progress.

4. Conclusion

In summary, using the octahedral-to-tetrahedral structure transition in ZnO buffer layer, polarity control of Zn-polar ZnO films was realized on rocksalt MgO (1 1 1) template. By RHEED observations and HRTEM characterizations, we established both the metastable rocksalt ZnO structure and the phase transition from octahedrally bonded rocksalt to tetrahedrally bonded wurtzite structure in ZnO buffer layer. For ZnO interfacial structures on RS-ZnO/RS-MgO template, the Zn–O bonds of Zn layer in rocksalt ZnO were proposed to firstly erect up to form the upright bonds, which directly results in the ZnO phase transition and the final achievement of Zn-polar ZnO.

Acknowledgments

This work is supported by the National Science Foundation (Grant nos. 60606023, 10804126, and 50532090), the Ministry of Science and Technology (Grant no. 2007CB936203, 2009CB929400) of China and Chinese Academy of Sciences.

References

[1] A. Tsukazaki, A. Ohtomo, T. Onuma, M. Ohtani, T. Makino, M. Sumiya, K Ohtani, S. Chichibu, S. Fuke, Y. Segawa, H. Ohno, H. Koinuma, M. Kawasaki, Nat. Mater. 4 (2005) 42.
[2] D.M. Bagnall, Y.F. Chen, Z. Zhu, T. Yao, S Koyama, M.Y. Shen, T. Goto, Appl. Phys. Lett. 70 (1997) 2230.
[3] R.E. Sherriff, D.C. Reynold, D.C. Look, B. Jogai, J.E. Hoelscher, T.C. Collins, G. Cantwell, W.C. Harsch, J. Appl. Phys. 88 (2000) 3454.
[4] S.H. Park, D. Ahn, Appl. Phys. Lett. 87 (2005) 253509.
[5] K. Koike, K. Hama, I. Nakashima, G. Takada, M. Ozaki, K. Ogata, S. Sasa, M. Inoue, M. Yano, Jpn. J. Appl. Phys. 43 (2004) L1372.
[6] H. Kato, K. Miyaamoto, M. Sano, T. Yao, Appl. Phys. Lett. 84 (2004) 4562.
[7] A. Tsukazaki, A. Ohtomo, K. Kita, Y. Ohno, H. Ohno, M. Kawasaki, Science 315 (2007) 1388.
[8] Y.F. Chen, S.K. Hong, H.J. Ko, V. Kirshner, T. Yao, Appl. Phys. Lett. 78 (2001) 3352.
[9] T. Minegishi, J.H. Yoo, H. Suzuki, Z. Vashaei, K. Inaba, K. Shim, T. Yao, J. Vac. Sci. Technol. B23 (2005) 1286.
[10] Y.F. Chen, S.K. Hong, H.J. Ko, T. Yao, Appl. Phys. Lett. 78 (2000) 559.
[11] Z.Q. Zeng, Y.Z. Liu, H.T. Yuan, Z.X. Mei, X.L. Du, J.F. Jia, Q.K. Xue, Z. Zhang, Appl. Phys. Lett. 90 (2007) 081911.
[12] S. Limpijumnong, S. Jungthawan, Phys. Rev. B 70 (2004) 054104.
[13] J.E. Jaffe, A.C. Hess, Phys. Rev. B 48 (1993) 7903.
[14] A. Zaoui, W. Sekkal, Phys. Rev. B 66 (2002) 174106.
[15] S. Desgreniers, Phys. Rev. B 58 (1998) 14102.
[16] H.T. Yuan, Y.Z. Liu, Z.Q. Zeng, Z.X. Mei, Y. Guo, P. Zhang, X.L. Du, J.F. Jia, Z. Zhang, Q.K. Xue, J. Cryst. Growth 311 (2009) 425.